

Linear cosmological perturbations in Scalar-tensor-vector gravity

Sara Jamali,^a Mahmood Roshan^{a,b} and Luca Amendola^c

^aDepartment of Physics, Ferdowsi University of Mashhad, P.O. Box 1436, Mashhad, Iran

^bSchool of Astronomy, Institute for Research in Fundamental Sciences (IPM), P.O. Box 19395-5531, Tehran, Iran

^cInstitute for Theoretical Physics, University of Heidelberg, Philosophenweg 16, D-69120 Heidelberg, Germany

E-mail: sara.jamali@mail.um.ac.ir, mroshan@um.ac.ir,
l.amendola@thphys.uni-heidelberg.de

Abstract. We investigate the cosmological perturbations in the context of a Scalar-Tensor-Vector theory of Gravity known as MOG in the literature. At the weak field limit, MOG increases the strength of gravity, and consequently addresses some astrophysical tests, without invoking dark matter particles. Recent investigations show that MOG reproduces a background cosmological evolution similar to Λ CDM, but with a matter dominated phase different from the standard case. In fact, the expansion rate in the matter dominated epoch is higher in MOG compared to that of Λ CDM. In this paper, in order to further investigate whether MOG passes the cosmological observations, we study the evolution of linear matter perturbations and estimate the modified gravity parameters. Unlike some current claims in the relevant literature, we show that MOG reduces the growth rate of the perturbations. We then compare MOG to the redshift space distortion (RSD) data. We find that MOG yields a much higher value than Λ CDM for the power spectrum parameter σ_8 . Although MOG cannot yet be ruled out by RSD data alone, the low growth and high σ_8 constitute a powerful challenge to the cosmological viability of MOG.

Contents

1	Introduction	1
2	The STVG theory	3
3	The perturbed equations	4
4	Perturbations in the sub-horizon scale	8
5	Comparison with observation	18
6	Discussion and Conclusion	20

1 Introduction

The Scalar-Vector-Tensor theory of gravity, also known as MOG in the literature, has been introduced by John W. Moffat [1]. MOG introduces two scalar fields, G and μ , and one vector field ϕ_α , in addition to the metric tensor. The existence of three extra fields implies some degrees of freedom by which MOG addresses the dark matter problem. It is well-known that this problem appears in different scales and systems like spiral galaxies, galaxy clusters and cosmological context. To address this problem, the astrophysical consequences of MOG have been widely investigated, for example, see [2]-[9].

In this paper, we focus on the cosmological behavior of the theory. Specifically, we are interested in the evolution of the scalar perturbations. MOG is considered as an alternative theory of gravity for dark matter, rather than dark energy. In fact, its extra fields cannot explain the cosmic speed up. To explain the accelerated expansion, MOG uses an effective cosmological constant Λ . Although in this theory Λ appears as a mass term for the scalar field G , and not as a standard cosmological constant, it is shown in [10] that the Λ term is responsible for the late time cosmic acceleration. On the other hand, in the absence of the cold dark matter component, it is natural to expect a different cosmological scenario in MOG governed by the extra gravitational fields. Using the dynamical system analysis in [10], the exact behavior of the extra fields in the cosmic history of the universe has been investigated. The evolution of the cosmos starts from a standard radiation dominated era, evolves toward a matter dominated epoch and tends to a late time accelerated phase. In [11], we investigated the cosmology of MOG at the background level and showed that MOG cannot fit the observational data of the angular size of the sound horizon; however, a slightly modified version of MOG, called mMOG, can solve the problem. The matter dominated era of mMOG is also slightly different from Λ CDM. In this case, it is necessary to study the linear cosmological perturbation in the matter dominated phase to shed light onto the viability of the theory. In this paper, we study the linear perturbations in both models MOG and mMOG.

It is claimed in the literature that MOG increases the growth rate of matter perturbations, compared to Λ CDM [12, 13]. Of course, this is the main feature that one might expect from a modified theory of gravity which aims to replace dark matter particles. In fact, an increase in the growth rate, compared to Λ CDM with the current density parameter

$\Omega_{m0} = 0.3$, is expected in order to compensate for the absence of dark matter. For an example for this point see [14]. This feature is an analog to what happens when we deal with the rotation curves in the weak field limit of the given modified gravity theory. Assuming a spherically symmetric matter distribution, one may simply write the rotational velocity outside the matter distribution as $v(r) = \sqrt{G_{\text{eff}}(r)M/r}$. Where G_{eff} is an effective Newtonian "constant" of gravitation and in principle, the modified gravity consequences appear in this function. On the other hand, we know that to explain the flat rotation curve data of spiral galaxies we need a mass component to raise the velocity curve in large distances. This means that, in the modified gravity approach, it is required to have $G_{\text{eff}(r)} > G$ at large distances from the center of the matter configuration. From this perspective, one may conclude that, at least in the weak field limit, a viable alternative gravity model for dark matter, should lead to a stronger gravitational force compared to the Newtonian case. Of course for theories that change the "dynamics" and not the gravitational sector, like the classic version of Modified-Newtonian-Dynamics (MOND), the above-mentioned description does not work.

However, recent studies on perturbations in MOG impose some assumptions which could restrict the generality of the final results. For example Refs. [12, 13] use the modified Poisson equation in MOG obtained in the weak field limit and in a non-expanding universe to study the linear perturbations. Furthermore, they simply ignore perturbations in some scalar fields. For example in [12] the scalar field G is assumed to be constant. Here we revisit the linear perturbations in MOG without putting any restrictive assumption. We present a complete description of the linear perturbations in all energy components. As we will show, our results are significantly different from the precedent analyses. More specifically, we do not confirm the main claim that MOG increases the growth rate of matter perturbations. Rather, we find a slower growth. Comparing to the available redshift space distortion (RSD) data, we find that in order to compensate the slower growth, the normalization σ_8 has to be substantially larger than in Λ CDM. Although *per se* this does not rule out MOG, such a high value will probably be in conflict with lensing and CMB results. We write down the full set of perturbation equations of MOG and derive the quasi-static limit. These equations can be used to address CMB and lensing data but a full treatment of this requires a complete reanalysis of the data and we leave it to future work. Concerning CMB, one could imagine that at early times MOG is corrected in some way to match CMB observations: in this case, only the late-time evolution will allow constraining or rule out the model.

This paper is organized as follow. In section 2 we briefly review the modified Friedmann equations of the theory. In section 3, we introduce the linear scalar perturbations in the metric, scalar and vector fields. We comprehensively investigate the perturbed field equations of the theory and, without imposing restrictive assumptions mentioned above, we find all the perturbed field equations in an expanding universe. Then we proceed to find the evolution of matter perturbations, as a key issue to compare the model with observations. In section 4 we apply the sub-horizon limit to the perturbed equations, and find the final equation governing the evolution of baryonic perturbations in the matter dominated era of MOG. We follow the same procedure for linear perturbations in mMOG. However, since the modified version, mMOG, has almost the same field equations, we do not repeat the calculations and present only the final results.

Using both analytical and numerical methods, we discuss all the features of the evolution of matter perturbations δ and growth rate function f . In section 5, applying the likelihood analysis of the RSD data for $f\sigma_8$, we find the best value of σ_8^0 for MOG and mMOG. The results are reported and discussed in section 6.

2 The STVG theory

Here is the action of Scalar-Tensor-Vector theory of Gravity known also as MOG [15]

$$S = S_{\text{gravity}} + S_{\text{scalar fields}} + S_{\text{vector field}} + S_{\text{m}} \quad (2.1)$$

in which,

$$S_{\text{gravity}} = \int \sqrt{-g} d^4x \left(\frac{R - 2\Lambda}{16\pi\mathcal{G}} \right) \quad (2.2)$$

$$S_{\text{scalar fields}} = \int \sqrt{-g} d^4x \frac{1}{2\mathcal{G}} g^{\mu\nu} \left(\frac{\nabla_\mu \mathcal{G} \nabla_\nu \mathcal{G}}{\mathcal{G}^2} + \frac{\nabla_\mu \mu \nabla_\nu \mu}{\mu^2} \right) \quad (2.3)$$

$$S_{\text{vector field}} = \int \sqrt{-g} d^4x \frac{1}{4\pi} \left(\frac{1}{4} B_{\mu\nu} B^{\mu\nu} + V_\phi \right) \quad (2.4)$$

where R is the Ricci scalar, Λ is the effective cosmological constant and the anti-symmetric tensor $B_{\mu\nu}$ is written as $\nabla_\mu \phi_\nu - \nabla_\nu \phi_\mu$ where ϕ_μ is the vector field. The Λ term can also be considered as the mass term for the scalar field \mathcal{G} . This term plays the same role to explain the cosmic speed-up [11] as the standard cosmological constant. Furthermore, the vector field's potential V_ϕ is set to $-\frac{1}{2}\mu^2\phi_\alpha\phi^\alpha$, in which μ , in general, is a scalar field which sets the mass of the vector field. This potential is the original form introduced in [1], that also leads to a viable weak field limit and also to an acceptable sequence of cosmic epochs. The action of matter, $S_{\text{m}}(g_{\alpha\beta}, \phi_\alpha)$, is postulated to be coupled to the vector field. In this case, there will be a non-zero fifth force current J_α . For the sake of simplicity and, as will appear more clearly later on, without loss of generality, we restrict ourselves to the case in which the scalar field μ is constant during the structure formation era. It should be mentioned that this scalar field does not play a crucial role in the cosmic history of MOG [16, 17]. More specifically it is shown in [11] and [10] that μ does not have a substantial contribution to the energy budget of the cosmos. On the other hand, the scalar field \mathcal{G} seriously influences the dynamics of the gravitating systems [2, 3]. It is useful to mention that, without μ , ϕ^α and Λ , MOG reduces to the Brans-Dicke scalar-tensor theory in its original form [18] with the dimensionless coupling constant $\omega_{BD} = -8\pi$. It is well known that in Brans-Dicke theory $\omega_{BD} \gg 1$ in order to pass the solar system observations. Therefore one may conclude that MOG cannot pass the classical tests in the absence of the vector field.

The energy-momentum tensors associated to the scalar field G and the vector field ϕ_α are defined in the following form

$$T_{\mu\nu(G)} = -\frac{2}{\sqrt{-g}} \frac{\delta S_G}{\delta g^{\mu\nu}} = -\frac{\nabla_\mu G \nabla_\nu G}{G} + \frac{1}{2} g_{\mu\nu} \frac{\nabla_\alpha G \nabla^\alpha G}{2G}, \quad (2.5)$$

$$T_{\mu\nu(\phi_\alpha)} = -\frac{2}{\sqrt{-g}} \frac{\delta S_\phi}{\delta g^{\mu\nu}} = -\frac{1}{4\pi} \left[B_\mu^\alpha B_{\nu\alpha} - g_{\mu\nu} \left(\frac{1}{4} B^{\rho\sigma} B_{\rho\sigma} + V_\phi \right) + 2 \frac{\partial V_\phi}{\partial g^{\mu\nu}} \right]. \quad (2.6)$$

where we have defined G as $G = 1/\mathcal{G}$. Now let us briefly review the field equations of the theory. Variation of the action (2.1) with respect to $g^{\mu\nu}$, yields the following modified Einstein equation

$$G_{\mu\nu} - \frac{\nabla_\mu \nabla_\nu G}{G} + g_{\mu\nu} \frac{\square G}{G} + \Lambda G g_{\mu\nu} = \frac{8\pi}{G} (T_{\mu\nu(G)} + T_{\mu\nu(\phi_\alpha)} + T_{\mu\nu(\text{m})}) \quad (2.7)$$

where $T_{\mu\nu(m)} = -\frac{2}{\sqrt{-g}} \frac{\delta S_m}{\delta g^{\mu\nu}}$ and $G_{\mu\nu}$ is the Einstein tensor. On the other hand, the following field equations can be derived by varying the actions (2.3) and (2.4) with respect to G and ϕ_α , respectively.

$$\square G = \frac{1}{16\pi} R G + \frac{1}{2G} \nabla_\alpha G \nabla^\alpha G - \frac{\Lambda G}{8\pi} \quad (2.8)$$

$$\nabla_\beta B^{\beta\alpha} = 4\pi J^\alpha - \mu^2 \phi^\alpha \quad (2.9)$$

where the d'Alembertian operator $\square G$ is defined as $\nabla_\alpha \nabla^\alpha G$, and the fifth force current is obtained by varying the matter action with respect to the vector field as $J^\alpha = \frac{1}{\sqrt{-g}} \frac{\delta S_m}{\delta \phi_\alpha}$. Now, using (2.8) and (2.9), we can establish the following continuity equations for G and ϕ_α

$$\nabla_\mu T^\mu_{\nu(\phi_\alpha)} = B_{\alpha\nu} J^\alpha - \frac{1}{4\pi} \frac{\partial V_\phi}{\partial \phi_\alpha} B_{\nu\alpha} + \frac{1}{4\pi} \nabla_\nu V_\phi - \frac{1}{2\pi} \nabla^\mu \left(\frac{\partial V_\phi}{\partial g^{\mu\nu}} \right), \quad (2.10)$$

$$\nabla_\mu T^\mu_{\nu(G)} = -\frac{R}{16\pi} \nabla_\nu G + \frac{\Lambda}{8\pi} \nabla_\nu G. \quad (2.11)$$

We suppose that the matter content of the universe is a perfect fluid. In this case provided that $\nabla_\alpha J^\alpha = 0$, which results in $\nabla_\alpha \phi^\alpha = 0$, one finds

$$\nabla_\alpha T^\alpha_{\nu(m)} = -B_{\alpha\nu} J^\alpha, \quad (2.12)$$

For more details on the derivation of this equation see [19]. It is worth mentioning that the assumption of isotropy and homogeneity in cosmology leads to $B_{\alpha\nu} = 0$ at the background level. Therefore using equation (2.12) one recovers the normal continuity equation for the ordinary matter in the context of MOG.

Now, we have the full set of equations to describe the dynamics of the cosmic fluid in the context of MOG. In the following section, we perturb them up to the first order and investigate the growth of density perturbations during the matter dominated era.

3 The perturbed equations

In this section, we introduce the linear perturbation equations. Let us start with the following perturbed metric in a flat space metric and in the Newtonian gauge

$$ds^2 = e^{2\tau} \left[- (1 + 2\Psi) \mathcal{H}^{-2} d\tau^2 + (1 + 2\Phi) \delta_{ij} dx^i dx^j \right] \quad (3.1)$$

where $\tau = \ln a$ is the conformal Hubble time or e -folding time, and $\mathcal{H} = Ha$ the conformal Hubble function. Conveniently, we deal with a single mode k , i.e. $\Psi = \Psi(\tau) e^{i\mathbf{k}\cdot\mathbf{r}}$ for the spatial part. One can write the perturbed fields G and ϕ_α as

$$\begin{aligned} G(\tau) &= G_0(\tau) + G_1(\tau) e^{i\mathbf{k}\cdot\mathbf{r}} \\ \phi_\alpha &= (\phi_\tau, \phi_i) = (\phi_{0\tau}(\tau) + \phi_{1\tau}(\tau) e^{i\mathbf{k}\cdot\mathbf{r}}, i k \phi_{1i}(\tau) e^{i\mathbf{k}\cdot\mathbf{r}}) \end{aligned} \quad (3.2)$$

where the subscript \mathbf{i} stands for any of three spatial components, i.e. (x, y, z) , and both background and perturbed quantities are functions of τ . From now on, the subscript 0 and 1 specifies the background and the first order perturbed fields, respectively.

Before moving on to perturb the field equations, we write the field equations (2.8) and (2.9) and the modified Friedmann equations¹ at the background level

$$\frac{G_0''}{G_0} = -\frac{G_0'\mathcal{H}'}{G_0\mathcal{H}} + \frac{G_0'^2}{2G_0^2} - \frac{2G_0'}{G_0} - \frac{3\mathcal{H}'}{8\pi\mathcal{H}} - \frac{3}{8\pi} + \frac{e^{2\tau}\Lambda}{8\pi\mathcal{H}^2}, \quad (3.3)$$

$$J_{0\tau}(\tau) = \frac{\mu^2\phi_{0\tau}}{4\pi} \quad (3.4)$$

$$\rho = (\mathcal{H}^2 e^{-2\tau}) \left(\frac{G'^2}{2G} + \frac{3G'}{8\pi} + \frac{3G}{8\pi} - \frac{G\Lambda}{8\pi\mathcal{H}^2 e^{-2\tau}} - \frac{\mu^2\phi_0^2}{8\pi} \right) \quad (3.5)$$

$$p = (\mathcal{H}^2 e^{-2\tau}) \left(-\frac{G'\mathcal{H}'}{8\pi\mathcal{H}} + \frac{G'^2}{2G} - \frac{G'}{8\pi} + \frac{G\Lambda}{8\pi\mathcal{H}^2 e^{-2\tau}} - \frac{G\mathcal{H}'}{4\pi\mathcal{H}} - \frac{G''}{8\pi} - \frac{G}{8\pi} - \frac{\mu^2\phi_0^2}{8\pi} \right) \quad (3.6)$$

where a prime stands for derivative with respect to τ . As we shall see, equations (3.3) and (3.4) are necessary to simplify the first order equations.

In the following we calculate the perturbed energy-momentum tensors already defined in section (2). Let us start with the ordinary energy-matter content of the universe, taken to be a perfect fluid, see [21] for more details

$$\begin{aligned} T_{0(m)}^0 &= -\left(\rho + \delta\rho e^{i\mathbf{k}\cdot\mathbf{r}}\right) \\ T_{0(m)}^i &= \frac{i}{\sqrt{3}k}\rho\theta(\omega+1)e^{i\mathbf{k}\cdot\mathbf{r}} \\ T_{i(m)}^j &= (\rho\omega + c_s^2\delta\rho e^{i\mathbf{k}\cdot\mathbf{r}}) + \Sigma_i^j \end{aligned} \quad (3.7)$$

where ω is the equation of state parameter, $\delta = \frac{\delta\rho}{\rho}$ is the density contrast, ρ is the background density, $\theta = i\mathbf{k}\cdot\mathbf{v}/\mathcal{H}$ is the velocity divergence and \mathbf{v} is the peculiar velocity. Perturbations in the fluid pressure p is $\delta p = c_s^2\delta\rho$, where c_s^2 is the adiabatic sound speed of the fluid. For perfect fluid, we ignore the anisotropic stress tensor Σ_i^j .

Similarly, in the following we linearize the energy-momentum tensors associated to fields G and ϕ_α . To do so, we use equation (2.5), and find the first order perturbation of $T_{(G)}^{\mu\nu}$ shown as $\delta T_{(G)}^{\mu\nu}$. The result is written as

$$\begin{aligned} \delta T_{0(G)}^0 &= -\delta T_{i(G)}^i = \frac{\mathcal{H}^2 G_0'}{2G_0^2} \left(2G_0(G_1' - \Psi G_0') - G_1 G_0' \right) e^{-2\tau+i\mathbf{k}\cdot\mathbf{r}} \\ \delta T_{0(G)}^i &= -\frac{ikG_1 G_0'}{\sqrt{3}G_0} e^{-2\tau+i\mathbf{k}\cdot\mathbf{r}} \end{aligned} \quad (3.8)$$

In a similar way, for the vector field ϕ_α , using equation (2.6), we have

$$\begin{aligned} \delta T_{0(\phi_\alpha)}^0 &= -\delta T_{i(\phi_\alpha)}^i = \frac{\mu^2 \mathcal{H}^2 \phi_{0\tau}}{4\pi} (\phi_{1\tau} - \phi_{0\tau}\Psi) e^{-2\tau+i\mathbf{k}\cdot\mathbf{r}} \\ \delta T_{0(\phi_\alpha)}^i &= \frac{ik}{4\pi} \mu^2 \phi_{1i} \phi_{0\tau} e^{-2\tau+i\mathbf{k}\cdot\mathbf{r}} \end{aligned} \quad (3.9)$$

Now we are ready to find the linearized form of the conservation equations (2.10) and (2.11). To do so, we first start with the scalar field G and use equations (2.11) and (2.5) to find the

¹For the modified Friedmann equations using FRW metric, see [11].

following first order relations. In this case the covariant derivative of (2.5) at the perturbed level gives

$$\begin{aligned}
\nabla_\mu \delta T_0^\mu{}_{(G)} &= G_1'' \frac{(\mathcal{H}^2 G_0')}{G_0} + G_1' \left(\frac{4\mathcal{H}^2 G_0'}{G_0} - \frac{3\mathcal{H}^2 (G_0')^2}{2G_0^2} + \frac{\mathcal{H}^2 G_0''}{G_0} + \frac{2\mathcal{H} G_0' H'}{G_0} \right) \\
&+ (G_0')^2 \left(\frac{3\mathcal{H}^2 \Phi'}{G_0} - \frac{\mathcal{H}^2 \Psi'}{G_0} \right) + \Psi \left(-\frac{2\mathcal{H}^2 G_0' G_0''}{G_0} + \frac{\mathcal{H}^2 (G_0')^3}{G_0^2} - \frac{4\mathcal{H}^2 (G_1')^2}{G} - \frac{2\mathcal{H} (G_0')^2 \mathcal{H}'}{G_0} \right) \\
&+ G_1 \left(-\frac{\mathcal{H}^2 G_0' G_0''}{G_0^2} + \frac{\mathcal{H}^2 (G_0')^3}{G_0^3} - \frac{2\mathcal{H}^2 (G_0')^2}{G_0^2} - \frac{\mathcal{H} (G_1')^2 \mathcal{H}'}{G_0^2} + \frac{k^2 G_0'}{G_0} \right), \\
\nabla_\mu \delta T_{\mathbf{i}}^\mu{}_{(G)} &= \frac{ik G_1 \mathcal{H}}{2\sqrt{3} G_0^2} (2G_0 (G_0' \mathcal{H}' + \mathcal{H} (G_0'' + 2G_0')) - \mathcal{H} G_0')^2 e^{-2\tau + i\mathbf{k} \cdot \mathbf{r}} \quad (3.10)
\end{aligned}$$

As equation (2.11) requires, we calculate the right hand side as

$$\begin{aligned}
\left(\frac{1}{16\pi} (R - 2\Lambda) \nabla_0 G \right)_1 &= -\frac{e^{-2\tau + i\mathbf{k} \cdot \mathbf{r}}}{8\pi} (3\mathcal{H} \mathcal{H}' (G_1' + G_0' (\Phi' - 2\Psi)) + k^2 G_0' (2\Phi + \Psi) - G_1' e^{2\tau} \Lambda \\
&+ 3\mathcal{H}^2 (G_1' + G_0' (\Phi'' + 3\Phi' - \Psi' - 2\Psi)) \\
\left(\frac{1}{16\pi} (R - 2\Lambda) \nabla_{\mathbf{i}} G \right)_1 &= -\frac{ik G_1}{8\pi \sqrt{3}} (3\mathcal{H} \mathcal{H}' + 3\mathcal{H}^2 - e^{2\tau} \Lambda) e^{-2\tau + i\mathbf{k} \cdot \mathbf{r}} \quad (3.11)
\end{aligned}$$

Now we equate the right-hand side of equations (3.10) and (3.11). The spatial component gives rise to a trivial relation. Notice that to show this point one needs to use the background equation for G_0'' given in (3.3). On the other hand, the time component leads to a second-order differential equation for G_1 , see equation (4.24). We will discuss more this relation in the next section.

Now we return to the vector field's conservation equation (2.10). Let us first use equation (3.9) and linearize the left hand side of equation (2.10). The result is

$$\begin{aligned}
\nabla_\mu \delta T_0^\mu(\phi_\alpha) &= 0 \\
\nabla_\mu \delta T_{\mathbf{i}}^\mu(\phi_\alpha) &= -\frac{ik \mu^2 \mathcal{H}^2}{12\pi} \phi_{0\tau} \left(\sqrt{3} \phi_{1\tau} - 3\phi'_{1i} \right) e^{-2\tau + i\mathbf{k} \cdot \mathbf{r}} \quad (3.12)
\end{aligned}$$

By keeping the first order terms in the right hand side of (2.10), one can easily show that the time component is zero. On the other hand, for the special component it turns out that except the first term in the right hand side, other terms do not have any contribute in the linear limit. Therefore the spatial component of the right hand side of (2.10) in the linear limit is written as

$$(B_{\alpha i} J^\alpha)_1 = -\frac{1}{3} ik \mathcal{H}^2 J_{0\tau} \left(\sqrt{3} \phi_{1\tau} - 3\phi'_{1i} \right) e^{-2\tau + ikr} \quad (3.13)$$

Now equating equations (3.12) and (3.13), and after summation over index \mathbf{i} , one may easily find the following scalar equation

$$ik \mathcal{H}^2 e^{-2\tau + i\mathbf{k} \cdot \mathbf{r}} (4\pi J_{0\tau} - \mu^2 \phi_{0\tau}) \left(\sqrt{3} \phi_{1\tau} - A_1' \right) = 0 \quad (3.14)$$

Where A_1 is $\sum_i \phi_{1i}$ and $A_1' = \sum_i \phi'_{1i}$. However equation (3.14) can not be considered as a new differential equation. More specifically using the vector field equation (2.9), one can readily conclude that the first parentheses vanishes, see equation (3.4). Notice that the second

parentheses is also zero. To prove it we use the field equation of ϕ_α . Let us take a divergence of (2.9) and take into account that $\nabla_\alpha \phi^\alpha = 0$ and $\nabla_\alpha J^\alpha = 0$. Therefore we have a constraint identity on $B_{\alpha\beta}$ as $\nabla_\alpha \nabla_\beta B^{\alpha\beta} = 0$. By linearizing this constraint we arrive at

$$(\mathcal{H}^5 - \mathcal{H})(f') + (6e^{2\tau}\mathcal{H}^3 - 4\mathcal{H}^4\mathcal{H}' - e^{2\tau}\mathcal{H}^2\mathcal{H}' - \mathcal{H}' + 4\mathcal{H}^5)f = 0 \quad (3.15)$$

where the function f is defined as $f = \sqrt{3}\phi_{1\tau} - A'_1$. One may straightforwardly conclude that $f = 0$. On the other hand, noting the cosmological principle one may conclude that $A = \phi_{1x} + \phi_{1y} + \phi_{1z} = 3\phi_{1j}$, where $j = 1, 2, 3$. This directly yields a simple differential equation between vector field components as

$$\phi'_{1j} = \frac{\phi_{1\tau}}{\sqrt{3}} \quad (3.16)$$

which is equivalent to $A'_1 = \sqrt{3}\phi_{1\tau}$ and consequently we have $\nabla_\mu \delta T^\mu_{\nu(\phi_\alpha)} = 0$, or equivalently $(B_{\alpha\nu}J^\alpha)_1 = 0$. This result has an interesting outcome. More specifically, as we have already mentioned, the ordinary matter energy-momentum tensor, in principle, is not conserved in MOG. However, in cosmology, at the background level, this tensor is conserved because of the isotropy and homogeneity of the cosmic fluid. In this case, the following usual conservation equation also hold in MOG

$$\rho' + 3(1 + \omega)\rho = 0. \quad (3.17)$$

where ω is the equation of state parameter. It is natural to expect that this conservation breaks down when dealing with first order perturbations. Nonetheless the above calculations show that $T^{\mu\nu}_{(m)}$ is conserved even in the linearized limit, i.e. $\nabla_\mu \delta T^\mu_{\nu(m)} = 0$, see equation (2.12). This conservation equation along with equation (3.7) leads to the following expressions

$$\delta k^2 c_s^2 + \mathcal{H}^2(\omega + 1)\theta' + \theta\mathcal{H}((\omega + 1)(\mathcal{H}(3\omega - 1) - \mathcal{H}') - \mathcal{H}\omega') - k^2\Psi(\omega + 1) = 0 \quad (3.18)$$

$$3\delta c_s^2 + \delta' + \theta + 3\Phi' - 3\delta w + \theta w + 3w\Phi' = 0 \quad (3.19)$$

where (3.18) is obtained from the spatial component $\nabla_\mu \delta T^\mu_{0(m)} = 0$, and (3.19) is the corresponding time component.

Now, let us summarize this section by considering the number of unknowns and the perturbation equations. We have seven unknown/perturbed quantities: G_1 , $\phi_{1\tau}$, ϕ_{1i} , ρ , θ , Ψ and Φ . Notice that we have assumed that all the spatial components of the vector field are equal. Accordingly, we need seven equations to describe the evolution of the perturbations. Therefore we used conservation equations and found three equations. More specifically, conservation equation of $T^{\mu\nu}_{(G)}$, i.e. equation (2.11) yields a differential equation for G_1 , see equation (4.24) in the next section. Furthermore, the conservation equation for $T^{\mu\nu}_{(m)}$ gives two differential equations (3.18) and (3.19). On the other hand, using the identity $\nabla_\alpha \nabla_\beta B^{\alpha\beta} = 0$ we found a relation between vector field components, see (3.16). Consequently, we still need three equations to construct a complete set of equations governing the first order perturbations. To find these three equations, in the next section we use the time component of the vector field equation (2.9), along with the off-diagonal and time components of the metric field equation (2.7).

4 Perturbations in the sub-horizon scale

In this section, we find the evolution of the density parameter δ in the sub-horizon scale. Specifically, the sub-horizon scale corresponds to scales in which the physical wavelength $2\pi a/k$ of perturbations is much smaller than the Hubble radius $1/H$. In order to apply the sub-horizon limit in the perturbed equations, we introduce the parameter $\lambda = \mathcal{H}/k \ll 1$. Then in the perturbation equations, we keep terms up to the lowest order of λ . Furthermore, notice that we restrict ourselves to the matter dominated epoch in MOG where the structure formation occurs. Therefore it is natural to expect that the equation of state parameter and the sound speed are zero, i.e. $\omega = 0$ and $c_s^2 = 0$.

Keeping these assumptions in mind, the off-diagonal component of (2.7), leads to the following relation

$$\Phi + \Psi = -\frac{G_1}{G_0} \quad (4.1)$$

Now, equation (3.19) can be written as

$$\delta' + 3(c_s^2 - \omega)\delta = -(\theta + 3\Phi')(\omega + 1) \quad (4.2)$$

On the other hand equation (3.18) gives

$$\theta' - \left(\frac{6\omega + 3\omega_t - 1}{2} - \frac{\omega'}{1 + \omega} \right) \theta = \frac{1}{\lambda^2} \left(\frac{c_s^2 \delta}{1 + \omega} + \Psi \right) \quad (4.3)$$

where we have conveniently defined the total equation of state parameter ω_t as follows

$$\frac{\mathcal{H}'}{\mathcal{H}} = 1 + \frac{H'}{H} = -\frac{1}{2} - \frac{3}{2}\omega_t. \quad (4.4)$$

Differentiating (4.2) with respect to $\tau = \ln a$, and combining with (4.3), one finds

$$\delta'' = \frac{1}{2}(3\omega_t - 1)(\delta' + 3\Phi') + \frac{1}{\lambda^2} \left(\frac{G_1}{G_0} + \Phi \right) - 3\Phi''. \quad (4.5)$$

As we already mentioned, in the sub-horizon limit, we ignore Φ'' and Φ' with respect to $\frac{\Phi}{\lambda^2}$. In order to find a relation between Φ and G_1 , we exploit the perturbed time component of equation (2.7)

$$\begin{aligned} \frac{\Phi}{\lambda^2} + \frac{\Lambda\Phi}{e^{-2\tau}\mathcal{H}^2} + \frac{1}{G_0} \left(G_1 \left(\frac{1}{2\lambda^2} + \frac{3}{2} - \frac{2\pi(G'_0)^2}{G_0^2} + \frac{e^{2\tau}\Lambda}{2\mathcal{H}^2} \right) + \left(\frac{4\pi G'_0}{G_0} + \frac{3}{2} \right) G'_1 - \frac{4\pi\rho(\delta + 2\Psi)}{e^{-2\tau}\mathcal{H}^2} \right. \\ \left. - \mu^2\phi_{0\tau}\phi_{1\tau} \right) = 0. \end{aligned} \quad (4.6)$$

Applying the sub-horizon limit for G , as we already did for Φ , equation (4.6) is simplified as

$$\frac{\Phi}{\lambda^2} + \frac{1}{G_0} \left(\frac{G_1}{2\lambda^2} - \frac{4\pi\rho\delta}{e^{-2\tau}\mathcal{H}^2} - \mu^2\phi_{0\tau}\phi_{1\tau} \right) = 0 \quad (4.7)$$

Now we need to find the last term $\mu^2\phi_{0\tau}\phi_{1\tau}$ in terms of the other perturbations. In order to quantify this term, we perturb the vector field equation (2.9). However for completeness, although it may seem trivial, let us first show that the constraints on J_α and ϕ_α , i.e. $\nabla_\alpha\phi^\alpha = 0$

and $\nabla_\alpha J^\alpha = 0$, do not add new first order equations for the vector fields. Let us start from the fifth force current J^α which is defined by [17]

$$J^\alpha = \kappa \rho_m u^\alpha \quad (4.8)$$

where u^α is the four-velocity, and ρ_m is the matter density. The metric (3.1) induces the following four velocity

$$u^\alpha = \frac{dx^\alpha}{ds} = \left(\frac{d\tau}{a(1+\Psi)\mathcal{H}^{-1}d\tau}, \frac{dx^i}{a\mathcal{H}^{-1}d\tau} \right) \approx \left(\frac{\mathcal{H}}{a}(1-\Psi), \frac{v^i}{a} \right) \quad (4.9)$$

In this way, the four-vector J^α takes the following form

$$J^\alpha = (J^0, J^i) = (e^{-\tau}\mathcal{H}\kappa\rho + \mathcal{H}\kappa\rho(\delta - \Psi)e^{-\tau+i\mathbf{k}\cdot\mathbf{r}}, -\frac{i\theta\mathcal{H}\kappa\rho}{\sqrt{3}k}e^{-\tau+i\mathbf{k}\cdot\mathbf{r}}) \quad (4.10)$$

where $\theta = \frac{i\mathbf{k}\cdot\mathbf{v}}{\mathcal{H}}$ and $\rho_m = \rho + \delta\rho e^{i\mathbf{k}\cdot\mathbf{r}}$. We then show that $\nabla_\alpha J^\alpha = 0$ does not impose new limitations at the linear level. Strictly speaking, the background level of this constraint leads to the usual continuity equation for matter,

$$e^{-\tau}\kappa\mathcal{H}(\rho' + 3\rho) = 0 \quad (4.11)$$

see for example equation (3.17). Similarly, at the perturbed level of $\nabla_\alpha J^\alpha = 0$, one finds

$$-e^{-\tau+i\mathbf{k}\cdot\mathbf{r}}\mathcal{H}\kappa\rho(\delta' + \theta + 3\Phi') = 0, \quad (4.12)$$

which recovers equation (4.2) for $\omega = c_s^2 = 0$. In fact, we were expecting this result since J^α is proportional to ρ_m and equations (4.11) and (4.12) are the continuity equation for matter at the background and perturbed level.

Now, we consider the field equation (2.9) at the linear level. Notice that we have already discussed it at the background level in equation (3.4). It is worth mentioning that one can use J^0 from equation (4.10) to rewrite equation (3.4) as

$$\phi_{0\tau} = \frac{4\pi\kappa\rho e^\tau}{\mathcal{H}\mu^2} \quad (4.13)$$

On the other hand, at the perturbed level, the time and spatial components of (2.9) can be written as

$$e^{i\mathbf{k}\cdot\mathbf{r}} \left(\sqrt{3}k^2 A'_1 - 24\pi\mathcal{H}^2\Psi J_{0\tau} + 12\pi\mathcal{H}^2 J_{1\tau} - 3\phi_{1\tau} (\mathcal{H}^2\mu^2 + k^2) + 6\mathcal{H}^2\mu^2\Psi\phi_{0\tau} \right) = 0 \quad (4.14)$$

$$-ike^{-2\tau+i\mathbf{k}\cdot\mathbf{r}} \left(\mathcal{H}^2 A''_1 + \mathcal{H}A'_1\mathcal{H}' - \sqrt{3}\mathcal{H}^2\phi'_{1\tau} - \sqrt{3}\phi_{1\tau}\mathcal{H}\mathcal{H}' + 4\pi\mathcal{J} - \mu^2 A_1 \right) = 0 \quad (4.15)$$

where $\mathcal{J} = \sum_i J_{1i}$. After some simple algebraic manipulations, using equation (3.16) and its derivative together with equation (4.13), and by taking into account that J^α is defined in equation (4.10), one finds the following equations from the time and spatial components, respectively

$$-3\mathcal{H}e^{i\mathbf{k}\cdot\mathbf{r}} (\phi_{1\tau}\mathcal{H}\mu^2 - 4\pi\kappa\rho e^\tau(\delta + \Psi)) = 0 \quad (4.16)$$

$$ie^{-2\tau+i\mathbf{k}\cdot\mathbf{r}} (4\sqrt{3}\pi\theta\mathcal{H}\kappa\rho e^\tau - k^2\mu^2 A_1) = 0. \quad (4.17)$$

which result in a simple relation for $\phi_{1\tau}$ and A_1 , respectively

$$\phi_{1\tau} = \frac{4\pi\kappa\rho e^\tau(\delta + \Psi)}{\mathcal{H}\mu^2}, \quad (4.18)$$

$$A_1 = \frac{4\sqrt{3}\pi\theta\mathcal{H}\kappa\rho e^\tau}{k^2\mu^2}. \quad (4.19)$$

Now, it is straightforward to show that $\nabla_\alpha\phi^\alpha = 0$ does not lead to a new constraint. At the background level this constraint is written as

$$\phi'_{0\tau} = -\frac{4\pi J_{0\tau}(\mathcal{H}' + 2\mathcal{H})}{\mathcal{H}\mu^2} = -\frac{4\pi\kappa\rho e^\tau(\mathcal{H}' + 2\mathcal{H})}{\mathcal{H}^2\mu^2} \quad (4.20)$$

It can be simply verified that equation (4.20) is the time derivative of (4.13). On the other hand, at the perturbed level, $\nabla_\alpha\phi^\alpha = 0$ gives

$$\begin{aligned} \sqrt{3}k^2 A_1\mu^2 - 24\pi\kappa\rho e^\tau\Psi(\mathcal{H}' + 2\mathcal{H}) + 3\mathcal{H}((\mathcal{H}' + 2\mathcal{H})\phi_{1\tau} + \mathcal{H}(\phi'_{1\tau} - 2\Psi\phi'_{0\tau})) \\ + 12\pi\mathcal{H}\kappa\rho e^\tau(3\Phi' - \Psi') = 0. \end{aligned} \quad (4.21)$$

Using equations (3.16), (4.13), (4.20) and (4.19), this equation takes the following simple form

$$12\pi\mathcal{H}\kappa\rho e^\tau(\delta' + \theta + 3\Phi') = 0 \quad (4.22)$$

which is equal to (4.12). Therefore we showed that $\nabla_\alpha\phi^\alpha = 0$ and equivalently $\nabla_\alpha J^\alpha = 0$ does not lead to new first order equations.

Now, let us return to equation (4.7) in which one can replace $\mu^2\phi_{0\tau}\phi_{1\tau}$, using equations (4.13) and (4.18). Moreover we ignore the term including Ψ when compared with $\frac{\Phi}{\lambda^2}$. Finally equation (4.7) takes the following form

$$\frac{\Phi}{\lambda^2} + \frac{1}{G_0} \left(\frac{G_1}{2\lambda^2} - \frac{4\pi\rho\delta}{e^{-2\tau}\mathcal{H}^2} - \left(\frac{4\pi\kappa\rho}{e^{-\tau}\mathcal{H}\mu} \right)^2 \delta \right) = 0 \quad (4.23)$$

In order to find the perturbed fields G_1 , Φ and Ψ , we require another relation. Therefore, as already mentioned, we use the time component of the conservation equation of $T_G^{\mu\nu}$, see (3.10) and (3.11). This equation is written as

$$\begin{aligned} G_1'' + G_1' \left(\frac{3}{2} - \frac{3\omega_t}{2} - \frac{G_0'}{G_0} \right) + G_1 \left(\frac{3}{16\pi} + \frac{G_0'^2}{2G_0^2} - \frac{9\omega_t}{16\pi} + \frac{1}{\lambda^2} + \frac{e^{2\tau}\Lambda}{8\pi\mathcal{H}^2} \right) - G_0'(\Psi' - 3\Phi') \\ + \frac{G_0}{4\pi\lambda^2} \left(\Phi + \frac{\Psi}{2} \right) + \frac{G_0}{16\pi} \left(15\Psi' - 9\omega_t\Phi' - 6\Psi' + 6\Psi'' + \frac{4\Lambda\Psi}{e^{-2\tau}\mathcal{H}^2} \right) = 0. \end{aligned} \quad (4.24)$$

In fact, we use this equation instead of the field equation of G given by (2.8). Keeping the lowest order of λ , (4.24) takes the following simple form

$$\frac{G_1}{\lambda^2} + \frac{G_0}{8\pi\lambda^2}(\Psi + 2\Phi) = 0 \quad (4.25)$$

Now, we have equations (4.1), (4.23) and (4.25) for three unknowns G_1 , Φ and Ψ . Some algebraic manipulations gives

$$\begin{aligned} \Psi &= -\frac{16\pi(4\pi - 1)\lambda^2\rho(4\pi\kappa^2\rho + \mu^2)}{(16\pi - 3)G\mathcal{H}^2e^{-2\tau}\mu^2}\delta \\ \Phi &= \frac{8\pi(8\pi - 1)\lambda^2\rho(4\pi\kappa^2\rho + \mu^2)}{(16\pi - 3)G\mathcal{H}^2e^{-2\tau}\mu^2}\delta \\ G_1 &= -\frac{8\pi\lambda^2\rho(4\pi\kappa^2\rho + \mu^2)}{(16\pi - 3)e^{-2\tau}\mathcal{H}^2\mu^2}\delta \end{aligned} \quad (4.26)$$

Then we have all the terms in (4.5) with respect to δ . As an aside, we notice that from these equations one can immediately derive the anisotropic stress $\eta = -\Phi/\Psi$

$$\eta = \frac{8\pi - 1}{8\pi - 2} \approx 1.04 \quad (4.27)$$

This quantity, which is unity in the standard case, can be measured by combining weak lensing and galaxy clustering, although present constraints are still very weak. In [20] it has been shown that a Euclid-like survey can measure a constant η to within a few percent. This might then be an additional way to distinguish MOG from standard gravity.

We focus from now on on the matter perturbation growth. In the context of MOG, the growth equation in the matter dominated era takes the form

$$\delta'' + \left(\frac{1}{2} - \frac{3\omega_t}{2}\right)\delta' - \frac{4\pi - 1}{16\pi - 3} \left(\frac{16\pi(4\pi\kappa^2\rho + \mu^2)}{G\mathcal{H}^2\mu^2 e^{-2\tau}}\right)\delta\rho = 0. \quad (4.28)$$

To simplify this equation, we first replace G_0 by $1/\mathcal{G}_0$, then ρ by $\frac{3\mathcal{H}^2 e^{-2\tau}\Omega_m}{8\pi\mathcal{G}_0}$ and the term $\mathcal{H}e^{-\tau}$ by H . Finally, we find

$$\delta'' + \left(\frac{1}{2} - \frac{3\omega_t}{2}\right)\delta' - \frac{(4\pi - 1)}{(16\pi - 3)} \left(\frac{6H^2\kappa^2\Omega_m}{\mathcal{G}_0\mu^2} + 4\right)\frac{3}{2}\Omega_m\delta = 0. \quad (4.29)$$

The coefficient

$$Y \equiv \frac{(4\pi - 1)}{(16\pi - 3)} \left(\frac{6H^2\kappa^2\Omega_m}{\mathcal{G}_0\mu^2} + 4\right) \quad (4.30)$$

represents the modification of the Poisson equation induced by MOG terms. One has $Y = 1$ in standard gravity. This coefficient is variously denoted as G_{eff} or μ in current literature. Together with η given above, it fully characterizes the theory at linear, quasi-static scales.

If we ignore the vector field (this can be simply done by setting κ to zero), then this equation recovers the corresponding equation in Brans-Dicke theory with $\omega_{BD} = -8\pi$, see equation (11.164) in [21]. This is not surprising as we already showed that in the absence of the vector field, MOG is equivalent to Brans-Dicke theory with $\omega_{BD} = -8\pi$. In order to simplify equation (4.29), let us review some results from [11], in which the following density parameters are introduced:

$$\begin{aligned} \Omega_m &= \frac{8\pi\mathcal{G}}{3H^2}\rho_m, & \Omega_r &= \frac{8\pi\mathcal{G}}{3H^2}\rho_r, & \Omega_\Lambda &= \frac{\Lambda}{3H^2} \\ \Omega_{\mathcal{G}} &= \frac{\mathcal{G}'}{\mathcal{G}} - \frac{4\pi}{3}\left(\frac{\mathcal{G}'}{\mathcal{G}}\right)^2, & \Omega_\mu &= -\frac{4\pi}{3}\left(\frac{\mu'}{\mu}\right)^2, \end{aligned} \quad (4.31)$$

Considering Fig. 1 and Table 1 in [11], it can be concluded that Ω_μ is almost negligible during the cosmic evolution of universe. This result confirms our previous assumption that the scalar field μ can be assumed constant in this analysis. Furthermore, one can clearly see that the cosmological constant does not contribute to the energy budget of matter dominated era. Now, using the modified Friedmann equations, see equation (3.2) in [11], one may write

$$\frac{12H^2\kappa^2\Omega_m^2}{\mathcal{G}_0\mu^2} = 1 - (\Omega_m + \Omega_R + \Omega_{\mathcal{G}} + \Omega_\Lambda) \quad (4.32)$$

combining equations (4.29) and (4.32), we arrive at

$$\delta'' + \left(\frac{1}{2} - \frac{3\omega_t}{2}\right)\delta' - \frac{3}{2}\Omega_m Y_{\text{MOG}}\delta = 0. \quad (4.33)$$

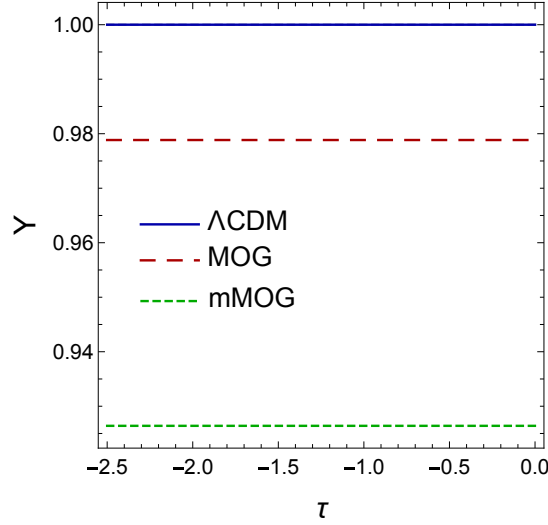


Figure 1. The evolution of the coefficients Y_{MOG} and Y_{mMOG} for $c = 0.33 \times 8\pi$ (see text) is compared to the ΛCDM case, i.e., the blue line $Y = 1$. The smaller Y for MOG and mMOG results in the slower growth rate.

where now we see that

$$Y_{\text{MOG}} = \frac{(4\pi - 1)}{2\Omega_m(16\pi - 3)} \left(1 - \Omega_R - \Omega_{\mathcal{G}} - \Omega_{\Lambda} + 7\Omega_m \right) \quad (4.34)$$

This is the main expression obtained in this paper to investigate the linear perturbations in MOG. It is clear that we need a numeric procedure to solve this equation. Before going through the numerical solution for equation (4.33), let us compare it with the corresponding equation in ΛCDM , namely

$$\delta'' + \left(\frac{1}{2} - \frac{3\omega_t}{2} \right) \delta' - \frac{3}{2}\Omega_m\delta = 0. \quad (4.35)$$

It is clear that the main difference between equations (4.33) and (4.35) is the coefficient Y , since ω_t evolves similarly in both MOG and ΛCDM , see [11] for more details. This coefficient can qualitatively specify whether the growth rate in MOG is smaller or larger than that of ΛCDM . Using numerical solutions presented in [11] for cosmic density parameters, Y has been shown in Fig. 1, for MOG, mMOG and ΛCDM . The value of Y in MOG and mMOG is smaller than ΛCDM . Therefore one may expect a slower growth rate for matter perturbations in MOG. This figure reveals another interesting feature. Although one may not expect it, Y in MOG and mMOG is also constant. One can easily verify that flat Y means that the left-hand side of (4.32) remains very small during the cosmic evolution. To be specific, let us write the left-hand side of equation (4.32) as follows

$$\xi \left(\frac{H}{H_0} \right)^2 \left(\frac{\mathcal{G}_N}{\mathcal{G}_0} \right)^2 \left(\frac{\mu_0}{\mu} \right)^2 \Omega_m^2 \quad (4.36)$$

where \mathcal{G}_N is Newton's gravitational constant, μ_0 is the current value of the scalar field μ and ξ is a dimensionless parameter defined as

$$\xi = \frac{\kappa^2 H_0^2}{\mathcal{G}_N \mu_0^2} = \frac{\alpha H_0^2}{\mu_0^2} \quad (4.37)$$

where $\alpha = \kappa^2/\mathcal{G}_N$. This parameter and μ_0 are two well-known parameters in MOG and their observational values are $\alpha \simeq 8.89$ and $\mu_0 \simeq 0.042 \text{ kpc}^{-1}$ [2, 3]. Using these values along with the current value of the Hubble parameter, we find

$$\xi \simeq 5.6 \times 10^{-10} h^2 \quad (4.38)$$

This very small value for ξ is the main reason for the flat behavior of Y . Let us write this condition, i.e., $\xi \ll 1$, as follows

$$\lambda_\phi \ll d_H \quad (4.39)$$

where $\lambda_\phi = 1/\mu_0$ is the Compton wavelength of the vector field and d_H is the Hubble distance. In other words, the length scale of the field is negligible compared with the cosmological Hubble length. This fact directly means that the vector field is not light enough to play a significant role in the cosmological scales. On the other hand, as we already mentioned, also the scalar field μ does not play an essential role in the cosmological background. Consequently, we can say that, in the cosmological context, the only important field of MOG is the scalar field G . In other terms, it seems that in the cosmological background, MOG is equivalent to a single scalar field Brans-Dicke theory. It is worthy to mention that unlike the screening fields, MOG's fields get hidden in the cosmological scales where the density is low, and get important in smaller scales as galaxies and galaxy clusters.

Keeping this primary result in mind, namely slow growth rates for matter perturbations in MOG, we investigate the numerical solution of (4.33), where for the background functions, i.e. $\omega_t(t)$ and Ω 's, we use the numerical solutions introduced in [11].

It is shown in [11] that the effective equation of state parameter in the matter dominated fixed point is $\omega_t = -0.01$. To obtain another crude comparison between the growth rates in standard description and MOG, let us simply assume that Ω 's are almost constant in the matter dominated universe (this assumption is not too restrictive, especially when we look at the matter dominated phase as a fixed point in the dynamical system approach), and rewrite (4.33) as follows

$$\delta'' + k_1 \delta' - k_2 \delta = 0 \quad (4.40)$$

The growing solution is written as

$$\delta \propto a^{\frac{1}{2}(\sqrt{k_1^2 + 4k_2} - k_1)} \propto t^{\frac{\sqrt{k_1^2 + 4k_2} - k_1}{3(1 + \omega_t)}} \quad (4.41)$$

In Newtonian case where $\omega_t = 0$ we have $k_1 = 1/2$ and $k_2 = 3/2$ (if $\Omega_m = 1$ in matter dominated phase), and consequently $\delta \propto a \propto t^{2/3}$. It is required that modified gravity theories aiming at replacing dark matter should increase the growth rate of density contrast in baryonic matter compared with the standard case. Therefore, in MOG we expect that $\sqrt{k_1^2 + 4k_2} - k_1 > 2(1 + \omega_t)$, or equivalently

$$k_2 > (1 + \omega_t)^2 + (1 + \omega_t)k_1 \quad (4.42)$$

On the other hand, in [11] the cosmology of MOG has been considered as a dynamical system. It has been shown that the matter dominated phase appears as a repulsive fixed point, called f_4 , in the dynamical system of the model. When the cosmological model reaches this fixed point in the phase space, we have $\omega_t = -0.01$, $\Omega_m \simeq 0.97$, $\Omega_G = 0.03$, $\Omega_R = 0$ and $\Omega_\Lambda = 0$. Using these data we arrive at $k_1 = 0.52$ and $k_2 = 1.42$. Therefore one may simply conclude that the condition (4.42) does not hold in MOG. Therefore our simple estimation shows that

although the scale factor grows close to the standard case, i.e. $a \propto t^{2/3}$, the matter contrast grows slower, as $\delta \propto t^{0.65}$, compared with the Newtonian case. This behavior seems completely against what one might expect from a modified theory of gravity aiming at replacing dark matter.

Now, let us solve (4.33) in a completely general way without restricting ourselves to the matter dominated era. To do so we use numerical solutions for Ω 's presented in [11], and keep all of them in our differential equation. Furthermore, we need to fix a suitable set of initial conditions. The simplest choice is to use the same initial conditions that is taken in deep matter dominated phase in Λ CDM, namely

$$\delta'(\tau^*) = \delta(\tau^*), \quad \delta(\tau^*) = a^*. \quad (4.43)$$

where the initial $\tau^* = \ln a^*$ is taken at $\tau = -2.5$, which corresponds to the redshift $z^* \simeq 11$. Here we show numerically that δ grows slower than in Λ CDM. This is clear from Fig. 2, in which the same initial condition for δ in MOG and Λ CDM are adopted. Notice that the initial conditions in modified theories of gravity, in principle, can be different from Λ CDM, for example see [22]. Consequently, we can try to change the first initial condition as

$$\delta'(\tau^*) = \beta \delta(\tau^*) \quad (4.44)$$

Starting from different initial conditions, i.e. with $\beta \neq 1$, we see from the right panel in Fig. 2 that we are soon back to the same evolution. Notice that, using our analytic solution, we find that at the deep matter dominated epoch $\delta'/\delta = (\sqrt{k_1^2 + 4k_2} - k_1)/2 < 1$. Therefore, we have studied $\beta < 1$, and concluded that the growth of δ in MOG is in all cases smaller than Λ CDM.

It is also instructive to investigate the growth rate parameter f of matter perturbations defined as follows

$$f = \frac{\delta'}{\delta} = \frac{d \ln \delta}{d \ln a} \quad (4.45)$$

In terms of f equation (4.33) can be written as

$$f' + f^2 + \frac{1}{2}(1 - 3\omega_t)f - \frac{3}{2}\Omega_m Y_{\text{MOG}} = 0. \quad (4.46)$$

To solve this equation, we need only one initial condition. So the initial condition (4.44), namely $f(z^*) = \beta$, is taken. The result has been illustrated in the right panel of Fig. (2). The solid blue and red curves belong to Λ CDM and MOG respectively. Dashed curves indicate f in MOG for different values of β . This panel clearly shows that the growth parameter f in MOG is always smaller than the standard case. It is interesting to mention that irrespective to the initial condition (β), the behavior of f does not change for $\tau > -1$. In fact if we perturb the initial condition, i.e. $\beta \rightarrow \beta + \delta\beta$, then the the growth rate will change as $f(\tau) \rightarrow f(\tau) + f_1(\tau)$. The above mentioned behavior means that $f_1(\tau)$ is a decreasing function of τ . Before discussing why this behavior is important to us, let us prove it using a simple first order stability analysis where $f_1 \ll f$. To do so, we use functions $k_1(\tau)$ and $k_2(\tau)$ defined in (4.40), and linearize equation (4.46) as follows

$$f_1' + (2f + k_1)f_1 = 0 \quad (4.47)$$

This equation can be simply integrated. The solution is written as

$$f_1 \propto e^{-\int^\tau (2f + k_1) d\tau}. \quad (4.48)$$

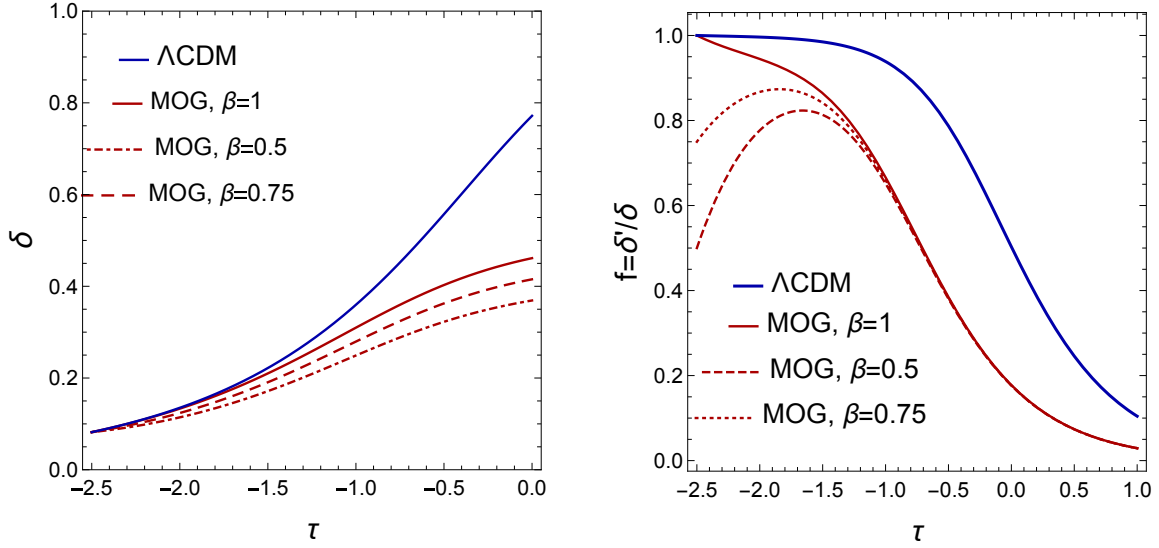


Figure 2. *left panel:* The evolution of δ in MOG and Λ CDM. The initial conditions for Λ CDM and MOG is $\delta(-2.5) = 0.082$ and $\delta'(-2.5) = \delta(-2.5)$. *right panel:* The growth rate function in MOG and Λ CDM with $f(-2.5) = 1$. By choosing different values for β in both figures, the tracking behavior for δ and f can be clearly seen.

On the other hand we know that $f > 0$ and $k_1(\tau) > 0$. Therefore it is clear that f_1 is a decreasing function of τ , and the evolution of the growth rate parameter is independent of the initial condition. We will see that this behavior plays a key role to determine the observational parameter $f\sigma_8^0$ in MOG.

Before starting the observational part where we find the best fit to the RSD data $f\sigma_8(z)$, let us check the growth rate in a different version of MOG, called as mMOG, introduced in [11]. A new parameter c has been incorporated by changing the kinetic energy contribution of the scalar field \mathcal{G} . In this case, one may find a much better agreement with the relevant sound horizon observations provided that the new parameter is fixed as $c \simeq 0.33 \times 8\pi$, see [11] for more details. Notice that one may recover MOG by setting $c = 8\pi$. For the sake of completeness, we consider c as a free parameter and investigate the evolution of matter perturbation δ and the growth parameter f in the context of mMOG. With completely similar calculations/analysis presented for MOG, we find the following equation for the linear perturbation δ

$$\delta'' + \left(\frac{1}{2} - \frac{3\omega_t}{2}\right)\delta' - \frac{3}{2}Y_{\text{mMOG}}\Omega_m\delta = 0. \quad (4.49)$$

where

$$Y_{\text{mMOG}} = \frac{(c-2)}{(8c-12)\Omega_m} \left(1 - \Omega_R - \Omega_G - \Omega_\Lambda + 7\Omega_m\right) \quad (4.50)$$

where $\Omega_G = \frac{\mathcal{G}'}{\mathcal{G}} - \frac{\varepsilon}{6}(\frac{\mathcal{G}'}{\mathcal{G}})^2$ and the rest of Ω 's are the same as in equation (4.31).

Before moving on to the numeric solution of the matter perturbations δ and the corresponding growth rate f in the matter dominated era of mMOG, let us present an analytic description. We consider a crude estimation that ω_t and Ω 's are constant. In this case, we are interested to see how δ in equation (4.49) is influenced by the new parameter c . Strictly speaking, we check whether the new constant c leads to a faster growth rate compared to the standard case. For our purpose, we need to substitute the matter dominated fixed point F_4 ,

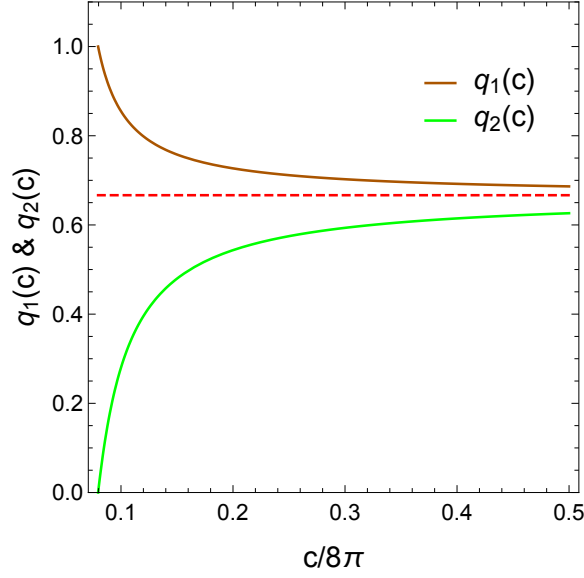


Figure 3. Evolution of q_1 and q_2 with respect to c where $a(t) \propto t^{q_1(c)}$ and $\delta \propto t^{q_2(c)}$. The curves smoothly reach the dashed green line which is the corresponding value for Λ CDM, i.e. $2/3$.

see Table 3 in [11], into the equation (4.49). In this case it is straightforward to show that the cosmic scale factor grows as $a(t) \propto t^{q_1(c)}$, where the function $q_1(c)$ is written as

$$q_1(c) = \frac{2(c-1)}{3c-4} \quad (4.51)$$

Furthermore equation (4.49) is integrated to give $\delta \propto t^{q_2(c)}$ where the function $q_2(c)$ is defined as

$$q_2(c) = \frac{\sqrt{50c^3 - 236c^2 + 370c - 192}}{2\sqrt{2c-3}(3c-4)} - \frac{c}{2(3c-4)} \quad (4.52)$$

It is clear that at the limit $c \rightarrow \infty$, both functions asymptotically reach to $2/3$. This means that expansion rate and the growth rate of the perturbations get identical to those of the standard cosmological model. In Fig. 3 we have plotted q_1 and q_2 in terms of the free parameter c , were for $c < 2$ there is a singularity in both functions. Moreover, these functions get negative, which is not interesting from the physical point of view. Therefore we have illustrated these functions for $c > 2$. Notice that in order to avoid the existence of a ghost in the theory, we have restricted ourselves to a positive c [11]. This figure reveals an interesting feature of the theory. More specifically, we see that irrespective to the magnitude of the free parameter c , $q_1(c) > 2/3$ and $q_2(c) < 2/3$. This means that this theory increases the expansion rate of the cosmos in the matter dominated phase, and accordingly decreases the perturbation growth rate. In other words, the effective impact is that the extra fields of the theory increase the expansion rate and decrease the matter perturbation growth. We already know that increasing the expansion rate, in principle, may reduce the matter growth. As an example, the Jeans analysis in a non-expanding isotropic and homogeneous fluid shows that matter perturbations grow exponentially with time. On the other hand in a similar situation, but in an expanding medium, matter perturbations grow as a power law function of time. For the special case $c = 0.33 \times 8\pi$ discussed above, we have $q_1 \simeq 0.7$ and $q_2 \simeq 0.6$. Therefore it seems that there is not a significant difference between MOG and mMOG as far as matter

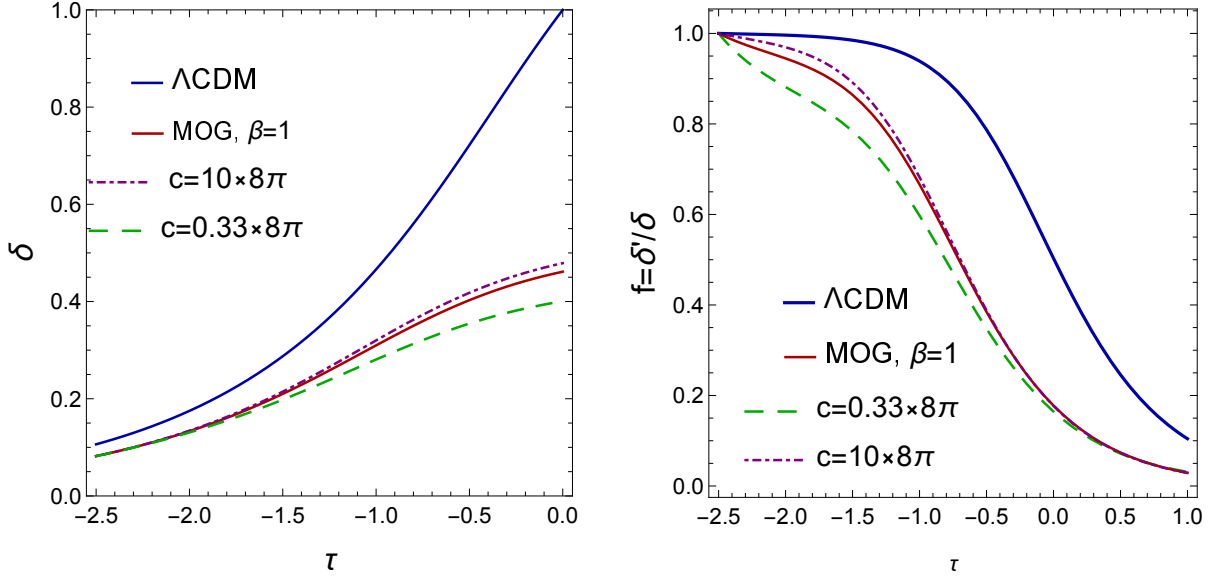


Figure 4. *left panel:* The evolution of δ in mMOG is smaller than Λ CDM for different choices of c . The initial conditions for Λ CDM and mMOG is $\delta'(-2.5) = \delta(-2.5)$ and $\delta(-2.5) = 0.082$. *right panel:* The behavior of f in mMOG and Λ CDM. The growth of perturbations in mMOG is smaller than Λ CDM, using the same initial condition, $f(-2.5) = 1$

perturbations are concerned. However, let us present the exact numeric solution of (4.49) for a similar set of initial conditions described for MOG. The result for different values of c has been shown in the left panel of Fig. 4. It is clear that the new parameter c does not lead to a significant deviation. However it is also clear that by decreasing c , we need a larger value for δ at the initial time to recover the current matter perturbation, i.e. $\delta = 1$.

The corresponding growth rate parameter f has been plotted in the right panel of Fig. 4. In this case it is easy to show that f satisfies the following first order differential equation

$$f' + f^2 + \left(\frac{1}{2} - \frac{3\omega_t}{2}\right)f - \frac{3}{2}Y_{\text{mMOG}}\Omega_m = 0. \quad (4.53)$$

The solutions for different values of c are shown in the right panel of Fig. 4. As we already discussed, there are minor differences between MOG and mMOG, and more importantly mMOG also can not lead to a larger growth rate for matter perturbations.

In summary, in this section, we considered the growth rate function f and the evolution of the matter perturbation δ in the framework of MOG and its slightly modified version, mMOG, based on numerical and analytical descriptions. We can simply conclude that this theory leads to slower matter growth compared to Λ CDM. This result is surprising in the sense that the usual Jeans analysis in a non-expanding infinite medium in MOG, leads to a smaller Jeans mass compared to the standard gravity. On the other hand, the growth rate of small perturbations is higher than the standard case [23]. This fact even happens in rotating systems, for more details see [7]. This behavior is natural in the sense that MOG increases the gravitational strength and consequently reduces the Jeans mass. However, one should note that at the cosmological level we deal with an expanding universe in which it is not trivial to simply characterize the impact of the extra fields on the growth rate of the perturbations. In this case, the growth depends also on the fraction of matter compared to other energy contributions. In other words, if the other homogeneous fields decrease this

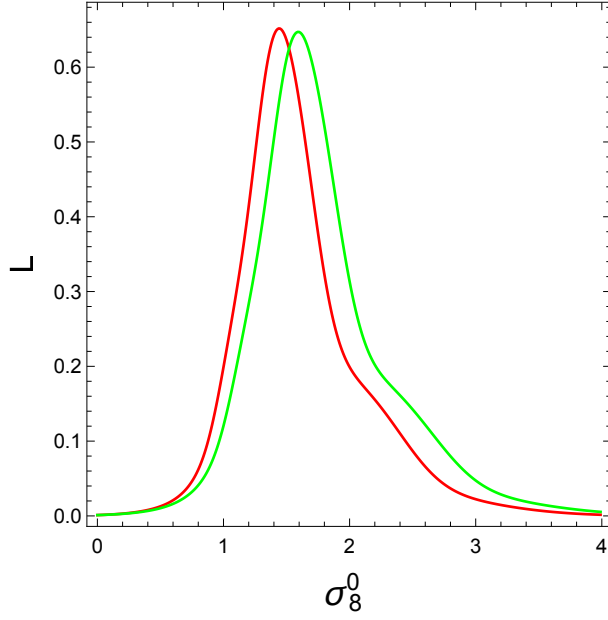


Figure 5. The likelihood analysis for MOG. The maximum values for MOG and mMOG correspond to $\sigma_8^0 = 1.44$ and 1.59 , respectively.

fraction, the effect might overcompensate the increase of gravitational strength, and the result is less growth.

In the following section, we compare our results with the relevant observation and discuss the viability of MOG as an alternative to dark matter particles.

5 Comparison with observation

In the previous section, we have found the evolution of the density perturbations δ and the growth function f in the context of MOG and a slightly modified version called mMOG. However as we already mentioned only the growth rate $f\sigma_8$ data is of observational importance and not the density contrast δ itself. Therefore here, we use the available data for $f\sigma_8$, also called the RSD observable, for comparing the main outcomes of (4.49) with observation. Notice that $f\sigma_8$ is defined as

$$f\sigma_8 \equiv \sigma_8(z) \frac{\delta'(z)}{\delta(z)} \quad (5.1)$$

in which the amplitude of the perturbations $\sigma_8(z)$ is conveniently defined as

$$\sigma_8(z) = \sigma_8^0 \frac{\delta(z)}{\delta(0)}. \quad (5.2)$$

To obtain the current value of σ_8 , it is necessary to specify the underlying gravity theory. Then σ_8^0 is determined through model dependent observations such as CMB power spectrum [24], weak lensing [25] and abundance of clusters [27]. Consequently, σ_8^0 is a model-dependent quantity [28], and naturally one may expect a different value for it in MOG compared with Λ CDM, where we have $\sigma_8^0 = 0.802 \pm 0.018$ [24]. In the following, we proceed along a simple

strategy. We assume that $f\sigma_8(z)$ data are also valid in MOG². Then we solve the perturbation equation (4.49), and by fitting to $f\sigma_8(z)$ data, we predict the best value for σ_8^0 in MOG. It is worth mentioning that the available data for $f\sigma_8$ lie in the redshift range $0 \leq z \leq 1.2$ (see Fig. 6). In this interval, the baryonic matter, the cosmological constant and the scalar field G have non-zero contribution to the energy budget of the Universe, see Fig. 1 in [11]. On the other hand, one can ignore radiation in equation (4.49).

As we already discussed, equation (4.33) needs two initial conditions to be solved. Consequently, we have two free parameters σ_8^0 and β . However, we have already shown in the previous section that the solution of equation (4.33) does not change significantly with initial conditions. In fact, there is a growing and a decaying mode, and the growing one wins, regardless of the initial conditions. Therefore, without loss of generality, we set $\beta = 1$ as in Λ CDM and find the best value of σ_8^0 .

The likelihood analysis can provide us with the best value of σ_8^0 to fit the RSD data. For the data points, \mathcal{D}_i , we used Table II in [29]. In the case of independent data points, the likelihood function \mathcal{L} is given by a simple relation,

$$\mathcal{L} = A \exp[-\chi^2/2] \quad (5.3)$$

in which A is a normalization constant and χ^2 is defined as

$$\chi^2 = \sum_i \frac{(\mathcal{D}_i - \mathcal{T}_i)^2}{\sigma_i^2} \quad (5.4)$$

where \mathcal{D}_i and \mathcal{T}_i refer to the predicted value of an observable by data and theory, respectively. Furthermore, σ_i is the error associated to the i th data point. Specifically, in our case, we have

$$\mathcal{L} = \sum_i A \exp\left[-\frac{1}{2}\left(\frac{\mathcal{D}_i(z) - \sigma_8^0 \times \mathcal{T}_i(z)}{\sigma_i}\right)^2\right]. \quad (5.5)$$

Results of the likelihood analysis for σ_8^0 are shown in Fig 5. The likelihood analysis reveals that the maximum of σ_8^0 is located at 1.44 and 1.59, for MOG and mMOG, respectively. It is worth mentioning that in MOG, one only considers the baryonic matter and in this regards, we expected a larger value for σ_8^0 , compared to Λ CDM, as also can be seen in [30].

Now, we can perform the last step of the comparison between data and theory. In Fig. 6, we plot $f\sigma_8$ for MOG, mMOG and Λ CDM along with the data points. We have shown the long-term evolution of $f\sigma_8$ for all the models, in the left panel of Fig. 6. We also fit a polynomial to the curves in MOG and mMOG. In the right panel, we restrict the plot to the available range of the data. In the case of Λ CDM we picked the reported σ_8^0 in [24], while for MOG and mMOG we used the result of our likelihood analysis. As the plot clearly shows, the evolution of $f\sigma_8$ in MOG and Λ CDM is significantly different. Although χ^2/dof is smaller in MOG, one needs more data points to decide which model can fit the data more accurately. The two curves of MOG and mMOG coincide and we almost get the same results.

We summarize all the results obtained from the likelihood analysis in Table 1. As expected, MOG and mMOG predict larger values for σ_8^0 . Of course, to make a reliable

²It is necessary to mention that the $f\sigma_8$ is not completely model independent and in principle, one has to find it for the model under consideration. In the case of MOG, we can use the available data points, since this theory is not going to change the whole paradigm of Λ CDM. In fact, MOG is designed to recover the same evolution for the background quantities as in Λ CDM without invoking the dark matter particles.

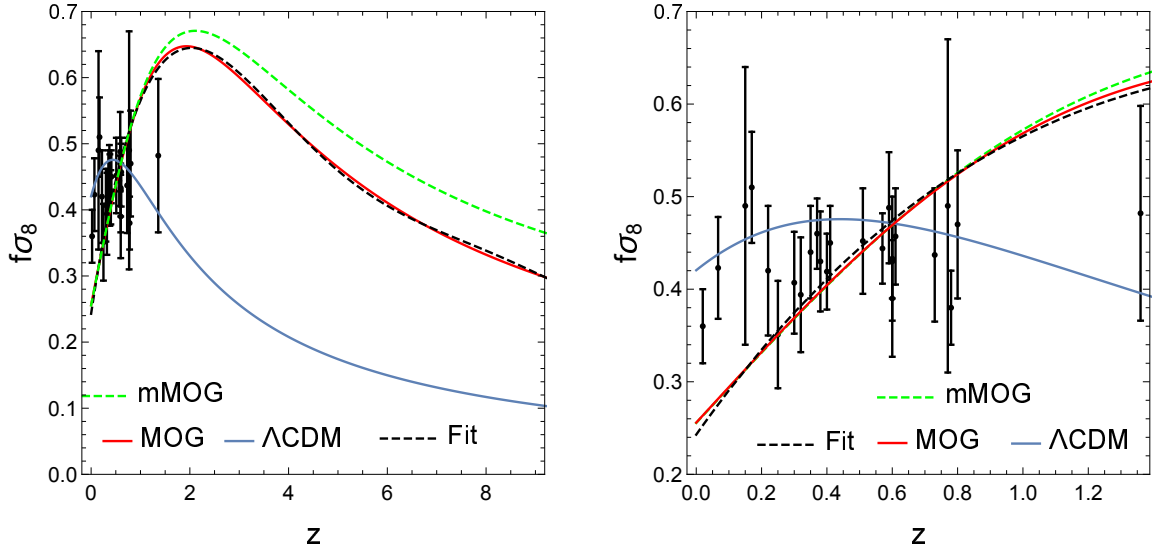


Figure 6. *left panel:* The evolution of $f\sigma_8^0$ for Λ CDM, mMOG with $c = 0.33 \times 8\pi$, MOG and best fit with the 5th order polynomial $\sum_k A_k a^k$, where $A_5 = 8 \times 10^{-5}$, $A_4 = -0.00275$, $A_3 = 0.03544$, $A_2 = -0.20970$, $A_1 = 0.49936$ and $A_0 = 0.24289$. *right panel:* The same as the right panel but zoomed into a smaller range of redshift.

decision on the viability of MOG as an alternative theory of dark matter, it is necessary to measure σ_8^0 from the relevant observations, like CMB and lensing [31] and compare it with that obtained in this paper. We leave this point for future studies. We know that in TeVeS, a relativistic version for Modified Newtonian Dynamics (MOND) [14], the extra vector field can play a role similar to cold dark matter [32] and increase the matter growth rate. However, our analysis shows that this is not the case in MOG, and the Proca vector field does not expedite the perturbation growth. Therefore, this point can be considered as a challenge to the viability of this theory.

6 Discussion and Conclusion

In this paper, we investigated the cosmological perturbations in the context of a Scalar-Tensor-Vector theory of gravity known as MOG in the literature. As in the standard case, we started from the modified Friedmann equations and introduced the perturbed metric in the Newtonian gauge. We assumed that the matter content of the universe is a perfect fluid, and without imposing restrictive assumptions on the evolution of the fields, found the first order perturbed field equations for linear scalar perturbations.

It is well known in the literature that any deviation from Λ CDM in matter dominated era may substantially influence the structure formation scenario. In order to consider this fact, we evaluated the evolution of matter perturbations, δ , and the growth function, $f = \delta'/\delta$, in the context of MOG. Since the growth of gravitational seeds starts in the sub-horizon scale, we have considered the perturbed equations in the sub-horizon limit in the matter dominated epoch.

In this way, we found the evolution of δ and f in the small-scale limit in the matter dominated era of MOG. We also presented a similar description for mMOG, which is a different version of MOG compatible with the sound horizon observations. Our solution reveals that the growth of matter perturbations in MOG is slower than in Λ CDM. In fact,

Λ CDM	MOG	mMOG
$\sigma_8^0=0.82$ [24]	$\sigma_8^0 = 1.44$	$\sigma_8^0 = 1.59$
$\chi^2/\text{dof}=0.703$	$\chi^2/\text{dof}=0.651$	$\chi^2/\text{dof}=0.647$

Table 1. σ_8^0 and χ^2/dof for Λ CDM, MOG and mMOG.

this is a surprising result, since in all the modified gravity theories aiming at replacing dark matter the gravitational force should be strengthened in the weak field limit, in order to explain the flat galactic rotation curves and other relevant issues. We wrote down the full set of perturbation equations and determined the two modified gravity parameters, η and Y . We then compared MOG, mMOG and Λ CDM with the observed $f\sigma_8$, and found that MOG and mMOG require higher values for σ_8^0 . The RSD data do not yet rule out MOG but the high value of σ_8 seems problematic when compared to recent estimates due to lensing. We conclude therefore that although MOG is not yet ruled out, a full analysis of CMB and lensing data will provide a strong challenge to MOG.

Acknowledgments

Sara Jamali thanks Henrik Nersisyan and Malihe Siavoshan for useful discussions. She also would like to thank the Institute for Theoretical Physics, University of Heidelberg for a very kind hospitality, during which some parts of this work have been done. Mahmood Roshan would like to thank Sohrab Rahvar for useful discussions.

References

- [1] J. W. Moffat, JCAP 0603, 004 (2006).
- [2] J. W. Moffat and S. Rahvar, Mon. Not. Roy. Astron. Soc. **441**, no. 4, 3724 (2014).
- [3] J. W. Moffat and S. Rahvar, Mon. Not. Roy. Astron. Soc. **436**, 1439 (2013).
- [4] N. Ghafourian and M. Roshan, Mon. Not. Roy. Astron. Soc. **468**, 4450 (2017).
- [5] J. R. Brownstein and J. W. Moffat, Mon. Not. Roy. Astron. Soc. **367**, 527 (2006).
- [6] M. Roshan, S. Abbassi and H. G. Khosroshahi, Astrophys. J. **832**, no. 2, 201 (2016).
- [7] M. Roshan and S. Abbassi, Astrophys. J. **802**, no. 1, 9 (2015).
- [8] M. Roshan, Astrophys. J. **854**, no. 1, 38 (2018).
- [9] N. S. Israel and J. W. Moffat, Galaxies **6**, no. 2, 41 (2018).
- [10] S. Jamali and M. Roshan, Eur. Phys. J. C **76**, no. 9, 490 (2016).
- [11] S. Jamali, M. Roshan and L. Amendola, JCAP **1801**, no. 01, 048 (2018).
- [12] F. Shojai, S. Cheraghchi and H. Bouzari Nezhad, Phys. Lett. B **770**, 43 (2017).
- [13] J. W. Moffat and V. T. Toth, Galaxies **1**, 65 (2013).
- [14] J. D. Bekenstein, Phys. Rev. D **70**, 083509 (2004).
- [15] J. W. Moffat and V. T. Toth, Class. Quant. Grav. **26**, 085002 (2009).
- [16] J. W. Moffat, arXiv : 1409.0853.
- [17] J. W. Moffat, arXiv : 1510.07037.

- [18] C. Brans and R. H. Dicke, Phys. Rev. **124**, 925 (1961).
- [19] M. Roshan, Phys. Rev. D **87**, 044005 (2013).
- [20] L. Amendola, S. Fogli, A. Guarnizo, M. Kunz and A. Vollmer, Phys. Rev. D **89**, no. 6, 063538 (2014); A. M. Pinho, S. Casas and L. Amendola, arXiv:1805.00027.
- [21] L. Amendola and S. Tsujikawa, Dark energy Theory and observation, (Cambridge University Press, 2010)
- [22] C. Di Porto and L. Amendola, Phys. Rev. D **77**, 083508 (2008).
- [23] M. Roshan and S. Abbassi, Phys. Rev. D **90**, no. 4, 044010 (2014).
- [24] P. A. R. Ade *et al.* [Planck Collaboration], Astron. Astrophys. **594**, A13 (2016).
- [25] S. More, H. Miyatake, R. Mandelbaum, M. Takada, D. Spergel, J. Brownstein and D. P. Schneider, Astrophys. J. **806**, no. 1, 2 (2015).
- [26] S. Alam *et al.* [BOSS Collaboration], Mon. Not. Roy. Astron. Soc. **470**, no. 3, 2617 (2017)
- [27] P. A. R. Ade *et al.* [Planck Collaboration], Astron. Astrophys. **594**, A24 (2016).
- [28] H. Nersisyan, A. F. Cid and L. Amendola, JCAP **1704**, no. 04, 046 (2017).
- [29] I. Albarran, M. Bouhmadi-Lopez and J. Morais, Phys. Dark Univ. **16**, 94 (2017).
- [30] N. MacCrann, J. Zuntz, S. Bridle, B. Jain and M. R. Becker, Mon. Not. Roy. Astron. Soc. **451**, no. 3, 2877 (2015).
- [31] H. Hildebrandt *et al.*, Mon. Not. Roy. Astron. Soc. **465**, 1454 (2017)
- [32] S. Dodelson and M. Liguori, Phys. Rev. Lett. **97**, 231301 (2006).